Journal of Heredity 2005:96(7):821–828
doi:10.1093/jhered/esi105
Advance Access publication September 8, 2005

Genes in Canine Articular Cartilage That Respond to Mechanical Injury: Gene Expression Studies With Affymetrix Canine GeneChip

N. Burton-Wurster, R. G. Mateescu, R. J. Todhunter, K. M. Clements, Q. Sun, V. Scarpino, and G. Lust

From the Baker Institute for Animal Health (Burton-Wurster, Clements, Mateescu, Scarpino and Lust); Department of Clinical Sciences (Todhunter), College of Veterinary Medicine, Cornell University, Ithaca, NY 14853; and Theory Center, Cornell University, Ithaca, NY 14853 (Sun). K. M. Clements is currently at AstraZeneca, Alderley Park, Macclesfield, Cheshire, UK SK10 4TG.

Address correspondence to N. Burton-Wurster, PhD, at the address above, or e-mail: niw1@cornell.edu.

Abstract

The Affymetrix canine GeneChip with 23,836 probe sets was used to look for cartilage genes that are significantly altered in response to mechanical impact. The model using canine articular cartilage explants loaded in vitro has been described previously (Chen et al., J Orthop Res 19:703–711, 2001). It is our hypothesis that genes that are activated or repressed in articular cartilage after impact injury initiate cartilage degeneration, leading to osteoarthritis in dogs. Gene expression of known cartilage genes was generally consistent with cartilage biology. A total of 528 genes were significantly ($P < .01$) up- or down-regulated in response to mechanical damage. After applying the strict Bonferroni correction, 172 remained significantly affected. One of these genes, MIG-6/gene 33, was chosen for verification by real- time quantitative reverse transcriptase polymerase chain reaction (RT-PCR). A 3.8- fold increase in expression was confirmed, consistent with the microarray chip data. Deficiencies in the current annotation of the canine chip are discussed. Gene expression studies with the Affymetrix canine GeneChip are potentially valuable, but await more complete annotation.

Of the more than 50 million dogs in the United States, 1 in 5 has osteoarthritis (OA), the hallmark of which is cartilage degeneration. Yet the origins of cartilage degeneration in canine OA are poorly understood and treatments for OA are mainly palliative. However, mechanical factors likely are involved. Thus instability resulting from cruciate ligament deficiency in the stifle and from developmental dysplasia of the hip is a major contributor to the pain and morbidity associated with OA.

A breeding colony of Labrador retrievers has been maintained at the Baker Institute for Animal Health since 1970. Members of this colony have been selectively bred for either a high or low occurrence of hip dysplasia. Much of the early work from this laboratory documents the accompanying OA (Lust and Pronsky 1972; Lust et al. 1972; Lust and Summers 1981). More recently, we have developed a special pedigree of dogs for genetic mapping obtained by crossing disease-free racing greyhounds with dysplastic Labrador retrievers (Bliss et al. 2002; Todhunter et al. 1999, 2003a,b). In our dogs with hip dysplasia, the cartilage degeneration that is observed can be related to subluxation of the hip leading to acetabular impingement on the femoral head at the site of lesion predilection (Burton-Wurster et al. 1999). Therefore, to better understand the relationship between mechanical factors and OA, we developed an in vitro model of mechanical damage that is now well characterized with respect to loading parameters and cellular and matrix responses, including cell death (Chen et al. 1999, 2001; Clements et al. 2004; Farquhar et al. 1996; Levin et al. 2001).

Although the etiopathogenesis of OA is unknown, there is evidence for an increase in the levels of chondrocyte death in osteoarthritic cartilage both in humans (Blanco et al. 1998) and in our canine hip dysplasia model (Burton-Wurster et al. 1982). This occurs alongside further damage to the cartilage matrix, including a decrease in the proteoglycan content (Brocklehurst et al. 1984), an increase in the water content

(Lust and Pronsky 1972; Maroudas and Venn 1977), an increase in fibronectin content (Burton-Wurster and Lust 1985), and an increase in the amount of collagen degradation (Burton-Wurster et al. 1982; Hollander et al. 1994). In vitro studies have reproduced these characteristic osteoarthritic changes using models of mechanical load and several studies have shown increased cell death postload (Chen et al. 2001; Farquhar et al. 1996; Levin et al. 2001; Loening et al. 2000; Lucchinetti et al. 2002). Work from our laboratory has shown that, over time, cell death spreads from the loaded to the surrounding, unloaded area of cartilage. When the central 2 mm of a 4 mm disc is loaded, initially dead cells are located in the region directly below the indenter. In loaded cartilage explants cultured for 21 days, cell death did not remain localized to the directly impacted region, but spread both radially and transversely into the surrounding ring cartilage. Furthermore, this spread could be prevented by physical separation and separate culture of the loaded and surrounding cartilage (Levin et al. 2001). These data suggest that a soluble factor is functioning as a messenger of cell death following mechanical loading. However, by conventional approaches, our data have eliminated one likely candidate, nitric oxide (NO), and determined that caspases do not play a role, thereby raising questions about the nature of the cell death involved (Clements et al. 2004).

Microarray technology is altering the way biologists can approach complex problems. Until now, the capacity for analysis was limited to one or a few genes or proteins at a time. The interest and expertise of the researcher and the availability of probes dictated the genes chosen for study. We are now at the opposite extreme. Many well- annotated human complementary DNA (cDNA) and oligonucleotide microarrays are available. Microarray data have been obtained from human patients with OA (Aigner et al. 2001). However, animal models using the dog permit the study of pathological changes much earlier than is possible using patient material. In vitro models permit us to address even more focused questions.

Affymetrix has produced the first commercially available canine expression array. The sequence information for this GeneChip canine genome array was obtained from GenBank (release 137.0, August 2003), dbEST (October 2003), and LION bioscience AG sequence information derived from cDNA libraries for 11 beagle tissues: testis, ovary, brain, embryo, liver, spleen, kidney, muscle, aorta, uterus, and jejunum. The Affymetrix canine GeneChip has 23,836 probe sets. We used this chip to look for genes that are significantly altered in response to mechanical damage or that are coregulated over time (cluster analysis). It is our hypothesis that genes that are activated or repressed in articular cartilage after mechanical impact initiate cartilage degeneration, leading to OA in dogs. In this article we present results obtained from the Affymetrix canine GeneChip and statistical analysis of the gene expression data to identify those genes that are up- or down-regulated in response to articular cartilage damage 24 h after impact loading. These candidate molecules are potentially responsible for the initiation and spread of matrix damage and cell death in impact damaged cartilage disks. The differential expression of one such candidate, novel to cartilage, has been validated by real-time quantitative reverse transcriptase polymerase chain reaction (qRT-PCR).

Materials and Methods

Cartilage Explants

Articular cartilage explants were obtained, as 4 mm discs, from canine shoulder joints, under sterile techniques, using a 4 mm biopsy punch and a no. 10 scalpel blade. The donor animals for the microarray experiment were F_1 backcrosses to the Labrador retrievers from the colony housed at the Baker Institute for Animal Health. The dogs, one male and one female, were 18 months old at the time of loading and three additional dogs, two male F_1 backcrosses to the Labrador and one full- bred Labrador female were necropsied at 2 years of age for the qRT-PCR experiment. Shoulders were macroscopically normal at the time of necropsy. The explants were washed three times with Gey's balanced salt solution (Sigma Chemicals, St. Louis, MO) and transferred to serum-free Ham's F12 medium (GIBCO, Carlsbad, CA) for culture. Medium was supplemented (per 100 ml) with 2.5 ml HEPES (1 M), 1.0 ml α-keto glutarate (3 mg/ml), 1.0 ml calcium chloride (4.85 g/ml), 200 μl gentamycin (10 mg/ml), 200 μl penicillin/streptomycin (10,000 U/ml Pen-G, 10,000 μg/ml streptomycin sulfate), and 400 μl Fungizone (250 μg/ml). After filtering through a 0.22 μm filter, this was supplemented with ITSCR+ premix (Collaborative Biosciences, Bedford, MA), and immediately before changing the media, it was supplemented with 1.0 ml L-glutamine (30 mg/ml) and 1.0 ml ascorbic acid (50 mg/ml). Explants were cultured for 48 h prior to loading at 37°C, 79% humidity, and 5% carbon dioxide.

Cyclic Impact Loading

Cyclic loads were applied to the central 2 mm of the 4 mm cartilage explants by means of a mechanical loading machine, which has been described previously (Chen et al. 1999; Farquhar et al. 1996). The loading machine allows pneumatically controlled testing of samples in triplicate while housed in an incubator. LabVIEW 6 programming software (National Instruments, Austin, TX) enables load control and data acquisition through a computer equipped with a PCI-M10-16E4 data acquisition board. Explants were loaded in stainless steel chambers and were held in place by stainless steel rings. The stainless steel indenters were nonporous. Loading chambers were filled with Gey's balanced salt solution for the duration of the loading. Loading was for 120 min at 5 MPa. The frequency of loading was 0.3 Hz, of which active loading lasted for 1.0 s per cycle. Loading in this square waveform produced a stress rate of 60 MPa/s. Control cartilage was kept in an identical metal chamber, but without loading. After loading, disks were placed in culture for 24 h and then frozen in liquid nitrogen in preparation for RNA extraction. Loaded and corresponding control disks were pooled separately for RNA extraction. For this initial microarray experiment, we had three biological replicates: three control pools (DB32-C1, DB52-C1, DB52-C2) and

three loaded pools (DB32-L1, DB52-L1, DB52-L2) with 12–16 disks per pool. Controls and loaded disks were carefully paired with respect to the site of origin on the humeral head and were loaded, or placed in loading chambers without load, at the same time on the same day. This experiment was repeated using cartilage from three additional dogs. RNA isolated from that cartilage was made available for qRT-PCR.

Isolation of RNA

RNA was isolated as described previously (MacLeod et al. 1996), but with two modifications. First, the pulverization step was omitted and cartilage was transferred directly to the homogenizer. This minimizes losses due to the small sample size. Second, the preparation was digested with RNase-free DNase while bound to the RNeasy columns (Qiagen, Valencia, CA). This results in a high- quality, DNA-free RNA preparation. We obtain consistently good yields (typically 400–800 ng RNA from 100 mg pooled cartilage disks) of pure, undegraded RNA with this protocol. For quantitation, RNA is measured in a fluorometric assay using SybrGreen II. The integrity of RNA can be viewed after electrophoresis in a formaldehyde/agarose gel (1.2% agarose with 0.74% formaldehyde) and staining with SYBR Green II.

Gene Expression on the Affymetrix Canine GeneChip

Purified RNA was sent to the University of Rochester microarray facility, where it was amplified and used to target the canine array. The quality of the RNA was checked again at Rochester on a bioanalyzer prior to amplification. The protocol that is described in detail in a technical bulletin by Affymetrix (GeneChip® Eukaryotic Small Sample Target Labeling Assay Version II; www.affymetrix.com) was used to amplify and label biotinylated cRNA. This protocol is important because cartilage is hypocellular with extensive matrix, making it difficult to obtain large amounts of RNA. With this method, ample RNA of high quality for multiple chips was obtained from the RNA we isolated and sent to the University of Rochester. Raw data were obtained with the high- density GeneChip Scanner 3000 at the University of Rochester. Initial analysis was performed using Gene Traffic through the University of Rochester server. Besides the gene annotations provided by Affymetrix, additional annotations were generated by BLASTX of the canine chip sequences against the National Center for Biotechnology Information (NCBI) nr database. The BLASTX analysis was performed on the Cornell Theory Center's parallel computer cluster. The updated Affymetrix annotation can be obtained on the Affymetrix Web sites: https://www.affymetrix.com/support/technical/byproduct.affx?product=canine and https://www.affymetrix.com/svghtml?query=#######_at. To improve the annotation quality for some of the Affymetrix sequences, longer sequence fragments from the dog genome project were used. The dog genome boxer sequences are available at http://www.ncbi.nlm.nih.gov/genome/guide/dog/.

Statistical Analysis

The statistical analysis was performed using GeneTraffic version 2.8, which uses a Student's *t* test for a standard two-class analysis and an *F* ratio for one-way analysis of variance (ANOVA) for multiple classes. The data were first subjected to variance stabilization using the same method as that used by the significance analysis of microarrays (SAM), developed at Stanford University, and available at http://www-stat.stanford.edu/~tibs/SAM/index.html. This method increases the precision for low expression values. Both the Benjamini-Hochberg (Benjamini and Hochberg 1995) and Bonferroni *P* value corrections were applied. The microarray hybridizations for the three loaded and paired control pools were performed at the same time. A paired *t* test was performed.

Real-Time qRT-PCR

In order to validate microarray data for the MIG-6 gene, qRT-PCR was performed with RNA from loaded and not loaded (control) cartilage using β-actin as an endogenous control. Canine-specific sequences for MIG-6 and β-actin were obtained from the Affymetrix Web sites (see above). PCR primers and TaqMan probes (Applied Biosystems, Foster City, CA) were designed using Primer Express version 1.0 software (Applied Biosystems) and are presented below:

MIG-6 forward	CCGGCGAGATTGGGACAGAG
MIG-6 reverse	GGGTCGGAACAGCAAAATCA
β-actin forward	ATGAACTCCCAGTCCTACGGG
β-actin reverse	TCCATGTCGTCCCAGTTGGT

TaqMan probes were labeled with a 3′,6-carboxy-tetramethylrhodamine (TAMRA, MIG-6) or VIC (β-actin) label as a quencher dye and a 5′,6- carboxyfluorescein label (6-FAM) as a reporter dye.

The 63 bp β-actin PCR product and the 67 bp MIG-6 PCR product were cloned into pCR II using Invitrogen's TA cloning kit. The plasmids were subsequently transfected into TOP10 competent cells (Invitrogen, Carlsbad, CA). Positive transformants were selected on the basis of kanamycin resistance. The canine cDNA structures for MIG-6 and β-actin were confirmed by sequencing. Large- scale plasmid DNA purification was carried out using a Qiagen plasmid kit. Both vectors were linearized by *Bam*HI and the cloned canine cDNAs were transcribed with T7 RNA polymerase at 37°C for 1 h using the reagents supplied with the Ambion's MaxiScript kit to produce sense MIG-6 and sense β-actin RNA. The concentration was calculated by absorbance at 260 nm.

A two-step, real-time qRT-PCR method was employed and real-time PCR was performed with the ABI Prism 7700 sequence detection system (Applied Biosystems). In the first step, sample total RNA or reference RNA (10 ng) were reverse transcribed in a volume of 10 μl containing TaqMan reverse transcription (RT) buffer, 5.5 mM $MgCl_2$, 500 μM each deoxynucleotide, 2.5 μM random hexamers, 0.4 U/μl RNase inhibitor, and 1.25 U/μl MultiScribe reverse

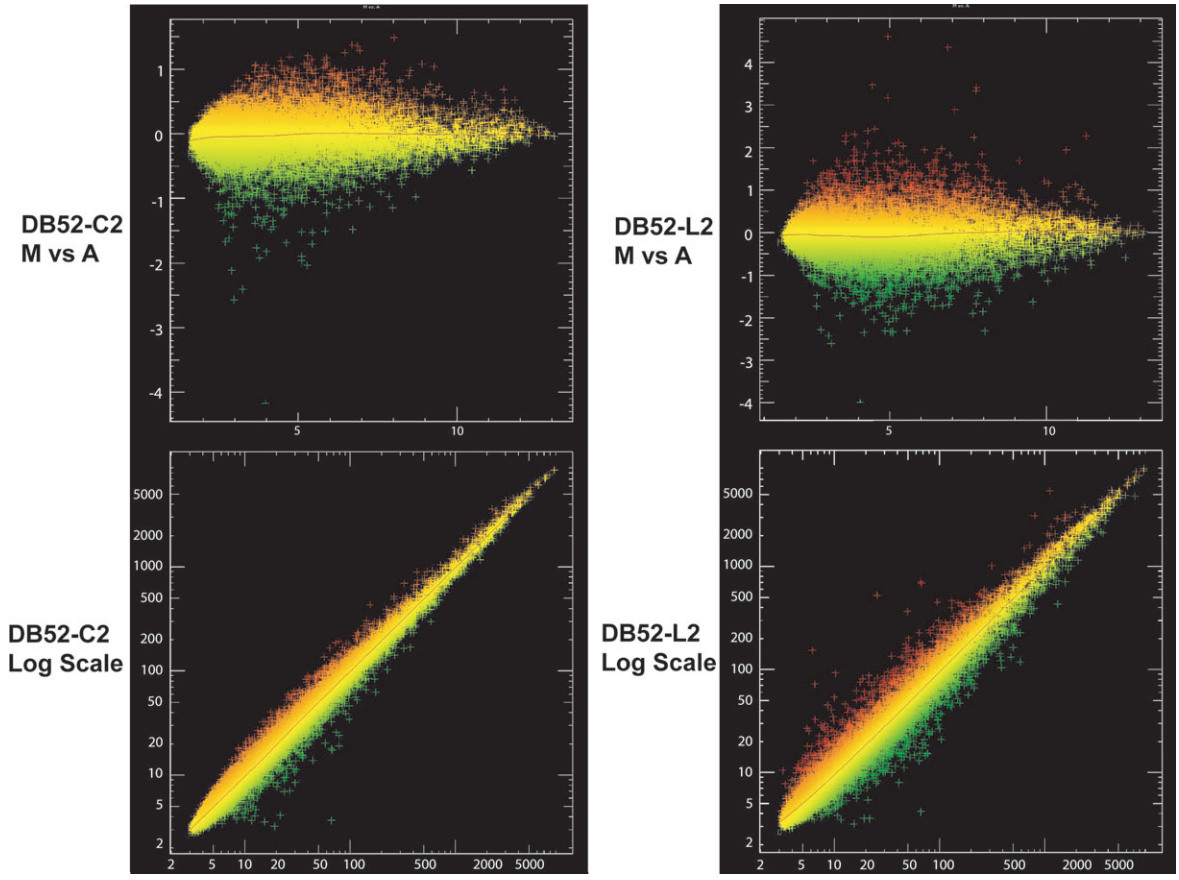

Figure 1. Scatter plots to assess microarray data. In the M versus A plot, the abscissa gives a measure of increasing signal intensity, $A = \log_2$ [(current chip × baseline)/2]. The ordinate, M, is the $\log_2$ ratio (current chip/baseline). The baseline is the average of the three controls. The plots show the desired relatively uniform distribution around $M = 0$ (red above, green below) as expected for a properly normalized dataset. The log scale plots make visible the greater changes in gene expression in the loaded (L2) than in the control (C2).

transcriptase at 25°C for 10 min, 48°C for 30 min, and 95°C for 5 min. In the second step, real-time PCR was carried out in a MicroAmp Optical 96-well plate (Applied Biosystems) using TaqMan Gold PCR reagents. Each well contained 1 µl of reverse transcribed cDNA, TaqMan buffer A, 5.5 mM $MgCl_2$, 200 µM each dATP/dCTP/dGTP, 400 µM dUTP, 900 nM each forward and reverse primers, 250 nM TaqMan probe, 0.01 U/µl AmpErase UNG (Applied Biosystems), and 0.025 U/µl AmpliTaq Gold DNA polymerase (Applied Biosystems) in a final volume of 25 µl. The thermal cycling conditions were the following: 50°C for 2 min, 95°C for 10 min, and 40 cycles of melting (95°C for 15 s), followed by annealing/extension (60°C for 60 s). In each qRT-PCR run, a standard curve for the target and the endogenous control gene was generated using a serial dilution reference RNA. Five-fold serial dilutions ranged from 0.001 pg to 0.16 pg of the standard cDNA fragment. Each sample was assayed in triplicate.

Absolute expression levels were determined by relating the measured threshold cycles (C_t) to the standard curve. Threshold cycles were defined as the number of PCR cycles at which the fluorescent signal reached a fixed threshold signal, being directly proportional to the amount of input.

Results

Figure 1 presents data from the hybridization statistics and supports the validity of the robust multichip analysis (RMA) normalization used. This is a conservative method and the option recommended in Gene Traffic.

We first wanted to determine if the gene expression data we were obtaining from the chip were consistent with known cartilage biology. Table 1 gives probe set data for a selection of genes that one would expect to find in cartilage. As expected, type II collagen and aggrecan were highly expressed genes, while type I collagen was absent. Decorin messenger RNA (mRNA) was detected with a 50- to 100- fold greater signal than biglycan, consistent with Cs-Szabó et al. (1997), who reported mRNA for decorin and biglycan to be present in adult human cartilage at a ratio of 158:8. Data are presented

Table 1. Signal intensities of genes relevant for cartilage

Probe ID	Gene	Grade	Avg. chip signal	Baseline signal	Call
1582388_at	Procollagen type II alpha 1	A	2611	2965	P
1582455_at	Preprocollagen type I, alpha 1	A	8	14	A/P
1582723_at	Collagen type I, alpha 2	A	12	29	A/P
1582466_at	Aggrecan precursor	A	1015	1472	P
1582724_at	Decorin	A	1917	2193	P
1582726_s_at	Decorin	A	3081	4211	P
1582437_at	Biglycan	A	42	44	A/P
1582799_s_at	Fibronectin	A	256	291	P
1582768_at	Fibronectin	A	218	295	P
1583017_at	Fibronectin ED-B	A	7	8	A/P
1582383_at	TIMP-1	A	2970	2396	P
1582708_at	TIMP-2	A	506	512	P
1582763_at	TNF-α	A	6	7	A
1582451_at	TGF-β	A	21	21	A/P
1582602_at	MMP3 stromelysin	A	795	876	P
1582770_at	MMP13 collagenase 3	A	17	22	A/P

for two different probe sets for decorin and for fibronectin. Data are also presented for the probe set for the ED-B isoform of fibronectin. A probe set with annotation for fibronectin isoform ED-A was identified, but the annotation was only a grade B, and a comparison with known sequence clearly showed that several of the chosen oligos were outside of the ED-A sequence. Therefore these data are not shown. Fibronectin probe set 1582799_s_at contains sequence coding within the III-14 segment, while 1582768_at contains sequence coding within the III-15 and I-10 segments. The former should detect all fibronectin isoforms, while the latter should be unable to detect the cartilage-specific isoform, which lacks the V, III-15, and I-10 segments (MacLeod et al. 1996). Theoretically it should detect about 50% fewer fibronectin mRNAs (Burton-Wurster et al. 1998). The mRNA for ED-B fibronectin should constitute about 10–20% of total fibronectin mRNA in cartilage (Burton-Wurster et al. 1989; Zhang et al. 1995), so the signal here was unexpectedly low.

A total of 528 genes were significantly ($P < .01$) up- or down-regulated in a paired *t* test with stabilization and the Benjamini-Hochberg correction. (Note: Gene Traffic version 3.2 identifies fewer significant genes on the same dataset—343 with no correction for multiple comparisons.) Table 2 presents these data as $\log_2$ ratios for a representative few genes for which annotation was achievable by the Cornell Theory Center from sequence provided by Affymetrix. The genes in bold type were still significant even after the stricter Bonferroni correction.

It should be noted that of 172 genes found significantly up- or down-regulated in a paired *t* test with stabilization and the Bonferroni correction, only 4 have received an annotation from Affymetrix, 3 with a grade A and 1 with a grade B. The three with grade A annotation are annexin A2, the Na and Cl-dependent taurine transporter, and tight junction protein 1 isoform a, which appear in Table 2. These were similarly identified by the Cornell search. For the remainder, no matches were found for 100, 20 matched to unknown proteins, and 48 matched to known proteins. For 28 of the known proteins, the calls by Affymetrix and by the Cornell search were in agreement; for 20, the calls were different.

Gene expression results from microarray data require verification. The gene with identification (ID) 153810_at was selected as the first gene to verify since it showed a greater than fourfold increase in expression, which was highly significant; it also showed up-regulation in an earlier feasibility experiment; its identification in the Cornell search as MIG-6,

Table 2. Selection of genes up- or down-regulated in impact-loaded cartilage explants

Mean $\log_2$ ratio	Gene	*P*
2.19	**MIG-6, gene 33**	<.00001
1.46	Prostaglandin E2 receptor EP3A	<.01>.00001
1.36	Integrin alpha 6 subunit	<.01>.00001
1.23	ATPase components of ABC transport	<.01>.00001
1.14	Karyopherin alpha 1 (importin)	<.01>.00001
0.92	Tubulin beta	<.01>.00001
0.86	**Annexin A2 (annexin II)**	<.01>.00001
0.77	Phenylalanine-tRNA synthetase beta	<.01>.00001
0.72	Mitochondrial ribosomal protein S26	<.01>.00001
0.71	**Dynein, cytoplasmic light chain**	<.01>.00001
0.56	**DNAJ (Hsp40) homolog, D, 1**	<.00001
0.48	**Cytochrome *c* oxidase**	<.00001
−0.41	**Alpha-1 catenin**	<.00001
−0.46	**Tight junction protein 1 isoform a; ZO-1**	
−0.57	**MAP kinase-activated protein. kinase 5**	<.00001
−0.69	**Mannose-6-phosphate/insulin-like-growth factor II receptor**	<.00001
−0.75	NADH dehydrogenase (ubiquinone) 1 beta subcomplex, 10	<.01>.00001
−0.85	**Na and Cl-dependent taurine transporter**	<.00001
−1.17	NADPH oxidase activator	<.01>.00001
−1.53	Fibroblast growth factor receptor 2	<.01>.00001

The genes in bold type were still significant even after the stricter Bonferroni correction.

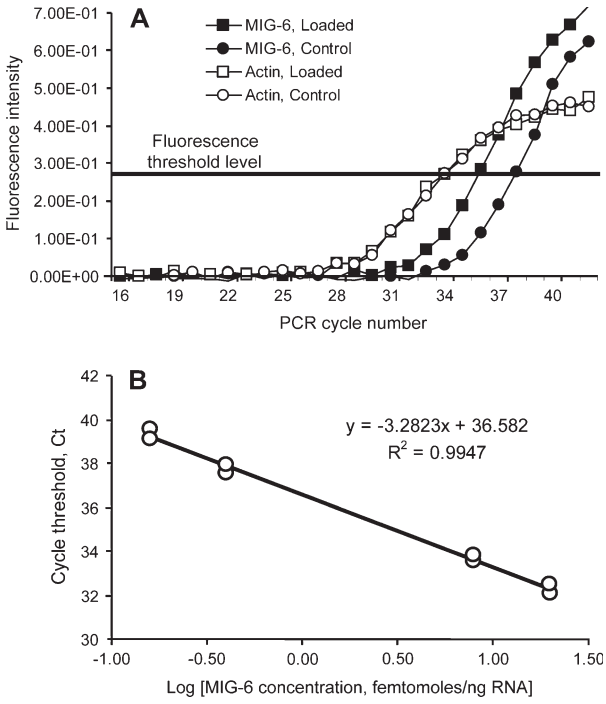

Figure 2. **(A)** Real-time PCR for MIG-6 and β-actin. The change in the emission intensity of the reporter dye divided by the emission intensity of a control reference dye after subtraction of the baseline is plotted against the PCR cycle number. The threshold is calculated as 10 times the standard deviation of the average signal of the fluorescent signal. **(B)** MIG-6 standard curve plot for the calculation of PCR efficiency and quantitation. A fivefold dilution of a control template is used to generate the standard curve. The resulting threshold cycle (C_t) values for each input amount of template are plotted as a function of the $\log_{10}$ concentration of input amounts and a linear trend line is fitted to the data. The resulting slope of the line fitted to the data is used to determine the PCR efficiency, as shown in the formula. An ideal slope should be 3.32 for 100% PCR efficiency. Optimal standard curves are based on PCR amplification efficiency from 90% to 100% (100% meaning that the amount of template is doubled after each cycle), as demonstrated by the slope of the standard curve equation. Linear regression analysis of all standard curves should show a high correlation (R^2 coefficient ≥ 0.99).

a gene responsive to stress, made biological sense in the context of the experiment; and it had not previously been reported in cartilage, so that results would add to our knowledge of cartilage biology. The gene for β-actin—IDs 1582488_at, 1582759_s_at, 1582760_x_at, 1582872_x_at—was chosen as a housekeeping gene. It showed little or no change in response to load (Figure 2A). The up-regulation of expression of gene MIG-6/gene 33 was confirmed by qRT-PCR. Typical real-time PCR data for one dog are shown in Figure 2A and a typical standard curve is shown in Figure 2B. The calculated fold increase for MIG-6 in loaded cartilage compared to the control cartilage was 3.88 ± 0.82 (n = 3), calculated from the real-time PCR quantification data presented in Table 3.

Table 3. Expression levels of MIG-6/gene 33 in impact-loaded and control cartilage

	Ct		Femtomoles/ng RNA		Loaded/ control
	Control	Loaded	Control	Loaded	
Dog1	37.10	34.89	0.70	3.27	4.67
Dog2	36.23	34.64	1.28	3.90	3.0
Dog5	36.88	34.95	0.81	3.15	3.89

Levels of MIG-6 and β-actin mRNA were generated from data and standard curves shown in Figure 2. MIG-6 mRNA levels adjusted for β-actin expression. Ct = number of threshold cycles.

Discussion

In our first experiment, a total of 528 genes were significantly ($P < .01$) up- or down-regulated in a paired t test with stabilization and the Benjamini-Hochberg correction. Of these, 248 (172 with a definitive call of "present") were still significantly affected, even after the stricter Bonferroni correction. Many of these genes have not been previously considered to have a role in OA. Some will be novel. For example, one gene identified and confirmed by qRT-PCR as significantly up-regulated four fold—MIG-6/gene 33—is known to respond to mechanical strain and other chronic stress stimuli (Makkinje et al. 2000). To our knowledge, its presence in cartilage has not been reported previously.

Gene expression of known cartilage genes was generally consistent with cartilage biology. The greatest challenge for investigators using this microarray remains the relatively poor status of annotation of the canine GeneChip. The gene identified as MIG-6/gene 33 has not been annotated by Affymetrix. Further, this is one of the genes for which Cornell and Affymetrix calls differ. However, the portion of the canine contig surrounding the target sequences for this gene contains most of the sequence for the human MIG-6/gene 33, with an apparent gap of 904 bases within the cDNA. This gap may be why the gene was not annotated by Affymetrix. A search of the Ensemble database (http://www.ensembl.org) reveals good alignment between human and canine sequences in the coding regions (462 and 453 amino acids, respectively), the last part of which contains a portion of the target sequence used to design the probe sets.

However, alignment between the canine target sequence and the human sequence falls off after this, perhaps another explanation for the failure to annotate. The ability to target genes within alternatively spliced regions should be a strength of using oligonucleotide probes. However, an examination of two of the genes with which we are familiar suggests that this strength is not realized. The probe 1582388_at was annotated as procollagen type IIA. This would imply that it is detecting the isoform of collagen that includes exon 2 and is rarely present in normal adult cartilage. In fact, the sequences

are not within exon 2 (Ryan and Sandell 1990), clearly are matched to the common sequences, and are detecting the procollagen type IIB found in cartilage, consistent with the relatively high level of expression observed. The probe identified as fibronectin ED-B was indeed within that alternatively spliced region; the probe identified as fibronectin ED-A included three probe sequences outside of the ED-A segment. There is no annotation to indicate that the other two fibronectin probe sets could distinguish between the cartilage-specific isoform and other isoforms. Uncritical use of the Affymetrix annotation would have given misleading results in these instances.

Based on our results, we consider gene expression studies with the Affymetrix canine GeneChip to be potentially very valuable. The presumption is that, as time goes on, the quantity and quality of the annotation will improve. Until then, investigators will need to exercise caution. However, the effort should be worthwhile. A more comprehensive understanding of the genes involved in the pathogenesis of OA and other diseases will open up new targets for therapeutic interventions and new candidates for the development of more efficient biomarkers. The identification of individuals in a preclinical phase will allow prophylactic interventions when they become available.

Acknowledgments

We thank Dr. Gene Hwang from the Department of Mathematics and Statistics at Cornell University for helpful discussions. We thank Brian Pan for excellent technical assistance and Dorothy Scorelle for assistance in the preparation of this manuscript. This work was supported by grants from Pfizer, Inc. and the Arthritis Foundation. An abstract of this article was delivered at the 2nd International Conference on the "Advances in Canine and Feline Genomics: Comparative Genome Anatomy and Genetic Disease," Universiteit Utrecht, Utrecht, The Netherlands, October 14–16, 2004.

References

Aigner T, Zien A, Gehrsitz A, Gebhard PM, and McKenna L, 2001. Anabolic and catabolic gene expression pattern analysis in normal versus osteoarthritic cartilage using complementary DNA-array technology. Arthritis Rheum 44:2777–2789.

Benjamini Y and Hochberg Y, 1995. Controlling the false discovery rate: a practical and powerful approach to multiple testing. J R Stat Soc B 57: 289–300.

Blanco FJ, Guitian R, Vázquez-Martul E, de Toro FJ, and Galdo F, 1998. Osteoarthritis chondrocytes die by apoptosis. Arthritis Rheum 41:284–289.

Bliss S, Todhunter RJ, Quaas R, Casella G, Wu R, Lust G, Williams AJ, Hamilton S, Dykes NL, Yeager A, Gilbert RO, Burton-Wurster NI, and Acland GM, 2002. Quantitative genetics of traits associated with hip dysplasia in a canine pedigree constructed by mating dysplastic Labrador retrievers with unaffected greyhounds. Am J Vet Res 63:1029–1035.

Brocklehurst R, Bayliss MT, Maroudas A, Coysh HL, Freeman MA, Revell PA, and Ali SY, 1984. The composition of normal and osteoarthritic articular cartilage from human knee joints. With special reference to unicompartmental replacement and osteotomy of the knee. J Bone Joint Surg Am 66:95–106.

Burton-Wurster N, Borden C, Lust G, and MacLeod JN, 1998. Expression of the $(V+C)^-$ fibronectin isoform is tightly linked to the presence of a cartilaginous matrix. Matrix Biol 17:193–203.

Burton-Wurster N, Farese JP, Todhunter RJ, and Lust G, 1999. Site-specific variation in femoral head cartilage composition in dogs at high and low risk for development of osteoarthritis: Insights into cartilage degeneration. Osteoarthritis Cartilage 7:486–497.

Burton-Wurster N, Hui-Chou CS, Greisen HA, and Lust G, 1982. Reduced deposition of collagen in the degenerated cartilage of dogs with degenerative joint disease. Biochim Biophys Acta 718:74–84.

Burton-Wurster N and Lust G, 1985. Deposition of fibronectin in articular cartilage of canine osteoarthritic joints. Am J Vet Res 46:2542–2545.

Burton-Wurster N, Lust G, and Wert R, 1989. Expression of the ED B fibronectin isoform in adult human articular cartilage. Biochem Biophys Res Commun 165:782–787.

Chen C-T, Burton-Wurster N, Borden C, Hueffer K, Bloom S, and Lust G, 2001. Chondrocyte necrosis and apoptosis in impact damaged articular cartilage. J Orthop Res 19:703–711.

Chen CT, Burton-Wurster N, Lust G, Bank RA, and Tekoppele JM, 1999. Compositional and metabolic changes in damaged cartilage are peak-stress, stress-rate and loading-duration dependent. J Orthop Res 17:870–879.

Clements KM, Burton-Wurster N, and Lust G, 2004. The spread of cell death from impact damaged cartilage: lack of evidence for the role of nitric oxide and caspases. Osteoarthritis Cartilage 12:577–585.

Cs-Szabó G, Melching LI, Roughley PJ, and Glant TT, 1997. Changes in messenger RNA and protein levels of proteoglycans and link protein in human osteoarthritic cartilage samples. Arthritis Rheum 40:1037–1045.

Farquhar T, Xia Y, Mann K, Bertram J, Burton-Wurster N, Jelinski L, and Lust G, 1996. Swelling and fibronectin accumulation in articular cartilage explants after cyclical impact. J Orthop Res 14:417–423.

Hollander AP, Heathfield TF, Webber C, Iwata Y, Bourne R, Rorabeck C, and Poole AR, 1994. Increased damage to type II collagen in osteoarthritic articular cartilage detected by new immunoassay. J Clin Invest 93:1722–1732.

Levin A, Burton-Wurster N, Chen C-T, and Lust G, 2001. Intercellular signaling as a cause of cell death in cyclically impacted cartilage explants. Osteoarthritis Cartilage 9:702–711.

Loening AM, James IE, Levenston ME, Badger AM, Frank EH, Kurz B, Nuttall ME, Hung H-H, Blake SM, Grodzinsky AJ, and Lark MW, 2000. Injurious mechanical compression of bovine articular cartilage induces chondrocyte apoptosis. Arch Biochem Biophys 381:205–212.

Lucchinetti E, Adams CS, Horton WE Jr, and Torzilli PA, 2002. Cartilage viability after repetitive loading: a preliminary report. Osteoarthritis Cartilage 10:71–81.

Lust G and Pronsky W, 1972. Glycosaminoglycan contents of normal and degenerative articular cartilage from dogs. Clin Chim Acta 39:281–286.

Lust G, Pronsky W, and Sherman DM, 1972. Biochemical and ultrastructural observations in normal and degenerative canine articular cartilage. Am J Vet Res 33:2429–2440.

Lust G and Summers BA, 1981. Early, asymptomatic stage of degenerative joint disease in canine hip joints. Am J Vet Res 42:1849–1855.

MacLeod JN, Burton-Wurster N, Gu DN, and Lust G, 1996. Fibronectin mRNA splice variant in articular cartilage lacks bases encoding the V, III-15 and I-10 protein segments. J Biol Chem 271:18954–18960.

Makkinje A, Quinn DA, Chen A, Cadilla CL, Force T, Bonventre JV, and Kyriakis JM, 2000. Gene 33/Mig-6, a transcriptionally inducible adapter protein that binds GTP-Cdc42 and activates SAPK/JNK: a potential marker transcript for chronic pathologic conditions, such as diabetic nephropathy. Possible role in the response to persistent stress. J Biol Chem 275: 17838–17847.

Maroudas A and Venn M, 1977. Chemical composition and swelling of normal and osteoarthritic femoral head cartilage. II. Swelling. Ann Rheum Dis 36:399–406.

Ryan MC and Sandell LJ, 1990. Differential expression of a cysteine-rich domain in the amino-terminal propeptide of type II (cartilage) procollagen by alternative splicing of mRNA. J Biol Chem 265:10334–10339.

Todhunter RJ, Acland GM, Olivier M, Williams AJ, Vernier-Singer M, Burton-Wurster N, Farese JP, Gröhn YT, Gilbert RO, Dykes NL, and Lust G, 1999. An outcrossed canine pedigree for linkage analysis of hip dysplasia. J Hered 90:83–92.

Todhunter RJ, Bliss SP, Casella G, Wu R, Lust G, Burton-Wurster NI, Williams AJ, Gilbert RO, and Acland GM, 2003a. Genetic structure of susceptibility traits for hip dysplasia and microsatellite informativeness of an outcrossed canine pedigree. J Hered 94:39–48.

Todhunter RJ, Casella G, Bliss SP, Lust G, Williams AJ, Hamilton S, Dykes NL, Yeager A, Gilbert RO, Burton-Wurster N, Mellersh CC, and Acland GM, 2003b. Power of a dysplastic Labrador retriever-greyhound pedigree for linkage analysis of hip dysplasia. Am J Vet Res 64: 418–424.

Zhang D, Burton-Wurster N, and Lust G, 1995. Alternative splicing of ED-A and ED-B sequences of fibronectin pre-mRNA differs in chondrocytes from different cartilaginous tissues and can be modulated by biological factors. J Biol Chem 270:1817–1822.

Corresponding Editor: Urs Giger